molecular pharmaceutics

articles

Effects of Experimental Setup on the Apparent Concentration Dependency of Active Efflux Transport in *in Vitro* Cell Permeation Experiments

Aki T. Heikkinen,*[,†,‡] Timo Korjamo,[§,∥] Varpu Lepikkö,[†,‡] and Jukka Mönkkönen[†,‡]

School of Pharmacy, Faculty of Health Sciences, University of Eastern Finland, Kuopio, Finland, Biocenter Kuopio, Kuopio, Finland, and Novamass Ltd, Oulu, Finland

Received December 14, 2009; Revised Manuscript Received February 8, 2010; Accepted February 17, 2010

Abstract: P-Glycoprotein mediated efflux is one of the barriers limiting drug absorption from the intestine. Predictions of the intestinal P-glycoprotein function need to take into account the concentration dependency because high intestinal drug concentrations may saturate P-glycoprotein. However, the substrate binding site of P-glycoprotein lies inside the cells and the drug concentration at the binding site cannot be measured directly. Therefore, rigorous determination of concentration dependent P-glycoprotein kinetics is challenging. In this study, the effects of the aqueous boundary layers, extracellular pH and cellular retention on the apparent saturation kinetics of P-glycoprotein mediated transport of quinidine in an *in vitro* cell permeation setting were explored. The changes in the experimental conditions caused 1 order of magnitude variation in the apparent affinity to P-glycoprotein ($K_{m,app}$) and a 5-fold difference in the maximum effective P-glycoprotein mediated transport rate of quinidine ($V_{max,app}$). However, fitting the concentration data into a compartmental model which accounted for the aqueous boundary layers, cell membranes and cellular retention suggested that the P-glycoprotein function *per se* was not altered, it was the differences in the passive transfer of quinidine which changed the apparent transport kinetics. These results provide further insight into the dynamics of the P-glycoprotein mediated transport and on the roles of several confounding factors involved in *in vitro* experimental setting. Further, the results confirm the applicability of compartmental model based data analysis approach in the determination of active transporter kinetics.

Keywords: P-Glycoprotein; permeability; *in vitro*−*in vivo* extrapolation (IVIVE); intestinal absorption; compartmental model

Introduction

In vitro cell monolayer permeation experiments can be used for the estimation of intestinal absorption potential of drug molecules.[1,2] A molecule's ability to permeate the cell monolayer in these *in vitro* experiments is often quantified by assuming that there is only a single barrier between the donor and receiver compartments.[3] However, it is well-known that the total permeation barrier in cell monolayer permeation experiments is made up of several individual barriers.[4] It has been demonstrated that, in addition to the intrinsic ability of the molecule to diffuse through the cellular structures, other factors, such as active transport, loss of sink conditions and cellular retention, can influence the apparent

* Corresponding author. Mailing address: School of Pharmacy, Faculty of Health Sciences, University of Eastern Finland, P.O. Box 1627, FIN-70211 Kuopio, Finland. Tel: +358 40 355 3465. Fax: +358 17 16 2252. E-mail: aki.heikkinen@uef.fi.

† University of Eastern Finland.

‡ Biocenter Kuopio.

§ Novamass Ltd.

∥ Current affiliation: R&D, Orion Corporation, Orion Pharma, Espoo, Finland.

(1) Artursson, P.; Palm, K.; Luthman, K. Caco-2 monolayers in experimental and theoretical predictions of drug transport. *Adv. Drug Delivery Rev.* **2001**, *46*, 27–43.

(2) Balimane, P. V.; Chong, S. Cell culture-based models for intestinal permeability: a critique. *Drug Discovery Today* **2005**, *10*, 335–343.

(3) Heikkinen, A. T.; Korjamo, T.; Mönkkönen, J. Modelling of Drug Disposition Kinetics in *In vitro* Intestinal Absorption Cell Models. *Basic Clin. Pharmacol. Toxicol.* **2010**, *106* (3), 180–188.

10.1021/mp9003089
Published on Web 02/17/2010

permeability. Nonetheless, the apparent permeability *in vitro* has been successfully used for prediction of intestinal absorption of passively absorbed compounds.[1] However, these predictions tend to be less reliable when the intestinal absorption is significantly affected by some transfer route other than passive transcellular diffusion, e.g. the paracellular route[5] or efflux transport.[6] Theoretically all the relevant transfer routes are involved in the cell monolayer permeation studies. However, a static *in vitro* cell model can never totally reflect the variation in the epithelial barrier occurring in the length of the intestine, and the relative role of different transfer routes in *in vitro* cell models are bound to differ from the *in vivo* setting. Therefore, a successful *in vitro*−*in vivo* extrapolation (IVIVE) of intestinal wall permeation requires a detailed mechanistic insight into the different transfer mechanisms involved in absorption. This, in turn, may require more sophisticated data analysis approaches than the traditional single-barrier view.[3]

P-Glycoprotein (P-gp/ABCB1) is an efflux transporter with a wide substrate specificity. Its substrates include several clinically important drugs, such as digoxin,[7] some HIV protease inhibitors[8] and anticancer agents.[9] P-gp has been shown to inhibit the intestinal absorption and access into the central nervous system as well as enhancing the hepatic and renal elimination of P-gp substrates.[10,11] Furthermore, P-gp mediated transport has also been suggested to contribute to the regulation of substrate concentration at the metabolic sites in the hepatocytes[12] and enterocytes.[13] Thus, P-gp may affect the pharmacokinetics of a wide range of compounds at several levels. In this respect, it is important to consider the contribution of P-gp when predicting the *in vivo* pharmacokinetics.

One of the key characteristics of P-gp mediated transport is its saturability; this is especially the case in the intestine where the drug concentrations are relatively high.[6,14,15] Thus, reasonable predictions of P-gp function *in vivo* must include the possibility of P-gp saturation. Usually the concentration dependency of P-gp mediated transport in *in vitro* cell permeation experiments is described via Michaelis−Menten type kinetics, i.e. with $V_{max,app}$ and $K_{m,app}$ parameters. In cell monolayer permeability experiments, these parameters have traditionally been estimated on the basis fo the observed apparent permeability (P_{app}) or the flux rate through the cell monolayer as a function of initial donor concentration (C_{d0}). However, the $V_{max,app}$ and $K_{m,app}$ parameters reported in the literature tend to vary significantly. This variability can partly be attributed to the fact that the binding site of P-gp lies within the cell monolayer,[16] whereas the concentration dependency is estimated on the basis of the initial donor concentration. Several factors in the experimental setup, in addition to initial donor concentration, can affect the local intracellular concentrations in the permeation experiments. Thus, it is reasonable to predict that these factors may affect also the apparent P-gp mediated transport.

Indeed, the effects of several factors on apparent P-gp mediated transport in permeation experiments have been discussed in the recent literature:

(A) In contrast to Michaelis−Menten theory, the $K_{m,app}$ values in the cell monolayer permeability assays have been reported to correlate with the $V_{max,app}$ value and, thus, also with the P-gp expression levels of the cells used.[17,18] This has been attributed to decreased substrate concentration at the binding site of P-gp due to the transporter function. Thus,

(4) Ho, N. F. H.; Raub, T. J.; Burton, P. S.; Barsuhn, C. L.; Adson, A.; Audus, K. L.; Borchardt, R. T. Quantitative Approaches to Delineate Passive Transport Mechanisms in Cell Culture Monolayers. In *Transport Processes in Pharmaceutical Systems*; Amidon, G. L., Lee, P. I., Topp, E. M., Eds.; Marcel Dekker Incorporated: New York, Basel, 1999; pp 219−316.

(5) Matsson, P.; Bergstrom, C. A.; Nagahara, N.; Tavelin, S.; Norinder, U.; Artursson, P. Exploring the role of different drug transport routes in permeability screening. *J. Med. Chem.* **2005**, *48*, 604–613.

(6) Li, C.; Liu, T.; Broske, L.; Brisson, J. M.; Uss, A. S.; Njoroge, F. G.; Morrison, R. A.; Cheng, K. C. Permeability evaluation of peptidic HCV protease inhibitors in Caco-2 cells-correlation with in vivo absorption predicted in humans. *Biochem. Pharmacol.* **2008**, *76*, 1757–1764.

(7) Englund, G.; Hallberg, P.; Artursson, P.; Michaelsson, K.; Melhus, H. Association between the number of coadministered P-glycoprotein inhibitors and serum digoxin levels in patients on therapeutic drug monitoring. *BMC Med.* **2004**, *2*, 8.

(8) Owen, A.; Chandler, B.; Back, D. J. The implications of P-glycoprotein in HIV: friend or foe. *Fundam. Clin. Pharmacol.* **2005**, *19*, 283–296.

(9) Schellens, J. H. M.; Malingré, M. M.; Kruijtzer, C. M. F.; Bardelmeijer, H. A.; van Tellingen, O.; Schinkel, A. H.; Beijnen, J. H. Modulation of oral bioavailability of anticancer drugs: from mouse to man. *Eur. J. Pharm. Sci.* **2000**, *12*, 103–110.

(10) Balayssac, D.; Authier, N.; Cayre, A.; Coudore, F. Does inhibition of P-glycoprotein lead to drug-drug interactions. *Toxicol. Lett.* **2005**, *156*, 319–329.

(11) Fromm, M. F. Importance of P-glycoprotein for drug disposition in humans. *Eur. J. Clin. Invest.* **2003**, *33* (2), 6.

(12) Lau, Y. Y.; Wu, C. Y.; Okochi, H.; Benet, L. Z. Ex situ inhibition of hepatic uptake and efflux significantly changes metabolism: hepatic enzyme-transporter interplay. *J. Pharmacol. Exp. Ther.* **2004**, *308*, 1040–1045.

(13) Knight, B.; Troutman, M.; Thakker, D. R. Deconvoluting the effects of P-glycoprotein on intestinal CYP3A: a major challenge. *Curr. Opin. Pharmacol.* **2006**, *6*, 528–532.

(14) Tubic, M.; Wagner, D.; Spahn-Langguth, H.; Bolger, M. B.; Langguth, P. In silico modeling of non-linear drug absorption for the P-gp substrate talinolol and of consequences for the resulting pharmacodynamic effect. *Pharm. Res.* **2006**, *23*, 1712–1720.

(15) Saitoh, R.; Miyayama, T.; Mitsui, T.; Akiba, Y.; Higashida, A.; Takata, S.; Kawanishi, T.; Aso, Y.; Itoh, Z.; Omura, S. Nonlinear intestinal pharmacokinetics of mitemcinal, the first acid-resistant non-peptide motilin receptor agonist, in rats. *Xenobiotica* **2007**, *37*, 1421–1432.

(16) Ambudkar, S. V.; Kim, I. W.; Sauna, Z. E. The power of the pump: Mechanisms of action of P-glycoprotein (ABCB1). *Eur. J. Pharm. Sci* **2006**, *27*, 392–400.

(17) Korjamo, T.; Kemilainen, H.; Heikkinen, A. T.; Mönkkönen, J. Decrease in intracellular concentration causes the shift in Km value of efflux pump substrates. *Drug Metab. Dispos.* **2007**, *35*, 1574–1579.

the extracellular substrate concentration needed to saturate the pump will be higher if more functional P-gp is being expressed in the cell monolayer used.[17,19,20]

(B) The pH of extracellular buffer has been shown to affect the apparent P-gp mediated transport of basic P-gp substrate quinidine in the rat *in situ* intestinal permeability assay.[21] As the pH of the extracellular buffer decreases, the apparent $V_{max,app}$ and $K_{m,app}$ increases because quinidine is more ionized at lower pH and consequently the ability to traverse the cell membrane to the binding site of P-gp is decreased.

(C) In addition to the cell monolayer, the aqueous boundary layer (ABL) on both sides of the cell monolayer may play a prominent role in the permeability barrier for high permeability compounds.[22,23] The effects of ABL on the apparent human apical sodium-dependent bile acid transporter (hASBT) kinetics have been examined recently.[24] Thus, it is likely that also apparent P-gp mediated efflux kinetics of high permeability substrates are affected by ABL.[17] However, no definitive data detailing this effect have been published.

(D) The majority of the P-gp substrates drugs are weak bases, and thus, it is possible that they are sequestered into the acidic intracellular compartments such as lysosomes.[25,26] Recently, it has been shown that lysosomal sequestration may significantly affect the apparent permeability.[27,28] Furthermore, lysosomal sequestration may affect the substrate concentration at the interaction site of P-gp. Thus, lysosomal sequestration is likely to affect the apparent P-gp mediated transport. Indeed, it has been reported that some lysosomotrophic agents can affect the apparent P-gp mediated transport in *in vitro* permeability experiments.[29] However, no definitive conclusions about the mechanism(s) underlying this finding can be drawn based on the data reported.

Although several factors affecting the apparent permeability of P-gp substrates and the apparent P-gp mediated transport are known, the relative contributions of these various factors are not fully understood. Consequently, it is not known how these factors should be taken into account when determining the concentration dependent P-gp function *in vitro* so that the parameters obtained could be used for valid prediction of saturation of intestinal P-gp *in vivo*.[30,31] However, a detailed dissection of the concentration dependent P-gp mediated transport would play a vital role in the successful IVIVE of intestinal P-gp function.[31,32]

In this study, we examined the effects of aqueous boundary layer, extracellular pH and lysosomal sequestration on the apparent P-gp mediated transport of quinidine. All these factors were demonstrated to affect the apparent P-gp mediated transport. Thereafter, a compartmental model was exploited to determine the concentration dependent P-gp mediated transport "*in situ*". This model takes into account the apical and basal cell membranes and aqueous boundary layers (ABL) separately and allows the discrimination of P-gp mediated transport from passive disposition processes. The current analysis provides further insight into the dynamics of the interplay of active transport and passive disposition through several barriers in cell monolayer permeation experiments. Furthermore, the implications on the IVIVE of active transport, especially in the context of intestinal absorption, are discussed.

(18) Shirasaka, Y.; Sakane, T.; Yamashita, S. Effect of P-glycoprotein expression levels on the concentration-dependent permeability of drugs to the cell membrane. *J. Pharm. Sci.* **2008**, *91*, 553–565.
(19) Bentz, J.; Tran, T. T.; Polli, J. W.; Ayrton, A.; Ellens, H. The steady-state Michaelis-Menten analysis of P-glycoprotein mediated transport through a confluent cell monolayer cannot predict the correct Michaelis constant Km. *Pharm. Res.* **2005**, *22*, 1667–1677.
(20) Sun, H.; Pang, K. S. Permeability, transport, and metabolism of solutes in Caco-2 cell monolayers: a theoretical study. *Drug Metab. Dispos.* **2008**, *36*, 102–123.
(21) Varma, M. V.; Panchagnula, R. pH-dependent functional activity of P-glycoprotein in limiting intestinal absorption of protic drugs: Kinetic analysis of quinidine efflux in situ. *J. Pharm. Sci.* **2005**, *94*, 2632–2643.
(22) Avdeef, A.; Artursson, P.; Neuhoff, S.; Lazorova, L.; Gråsjö, J.; Tavelin, S. Caco-2 permeability of weakly basic drugs predicted with the double-sink PAMPA pKa(flux) method. *Eur. J. Pharm. Sci.* **2005**, *24*, 333–349.
(23) Korjamo, T.; Heikkinen, A. T.; Mönkkönen, J. Analysis of unstirred water layer in *in vitro* permeability experiments. *J. Pharm. Sci.* **2009**, *98*, 4469–4479.
(24) Balakrishnan, A.; Hussainzada, N.; Gonzalez, P.; Bermejo, M.; Swaan, P. W.; Polli, J. E. Bias in estimation of transporter kinetic parameters from overexpression systems: Interplay of transporter expression level and substrate affinity. *J. Pharmacol. Exp. Ther.* **2007**, *320*, 133–144.
(25) Asokan, A.; Cho, M. J. Exploitation of intracellular pH gradients in the cellular delivery of macromolecules. *J. Pharm. Sci.* **2002**, *91*, 903–913.
(26) Duvvuri, M.; Krise, J. P. A novel assay reveals that weakly basic model compounds concentrate in lysosomes to an extent greater than pH-partitioning theory would predict. *Mol. Pharmacol.* **2005**, *2*, 440–448.
(27) Hayeshi, R.; Masimirembwa, C.; Mukanganyama, S.; Ungell, A. L. Lysosomal trapping of amodiaquine: impact on transport across intestinal epithelia models. *Biopharm. Drug Dispos.* **2008**, *29*, 324–334.
(28) Heikkinen, A. T.; Mönkkönen, J.; Korjamo, T. Kinetics of Cellular Retention during Caco-2 Permeation Experiments: Role of Lysosomal Sequestration and Impact on Permeability Estimates. *J. Pharmacol. Exp. Ther.* **2009**, *328*, 882–892.
(29) Lacave, R.; Ouar, Z.; Paulais, M.; Bens, M.; Ricci, S.; Cluzeaud, F.; Vandewalle, A. Lysosomotropic agents increase vinblastine efflux from mouse MDR proximal kidney cells exhibiting vectorial drug transport. *J. Cell. Physiol.* **1999**, *178*, 247–257.
(30) Del Amo, E. M.; Heikkinen, A. T.; Mönkkönen, J. In vitro-in vivo correlation in p-glycoprotein mediated transport in intestinal absorption. *Eur. J. Pharm. Sci.* **2009**, *36*, 200–211.
(31) Bolger, M. B.; Lukacova, V.; Woltosz, W. S. Simulations of the Nonlinear Dose Dependence for Substrates of Influx and Efflux Transporters in the Human Intestine. *AAPS J.* **2009**, *11*, 353–363.
(32) Badhan, R.; Penny, J.; Galetin, A.; Houston, J. B. Methodology for development of a physiological model incorporating CYP3A and P-glycoprotein for the prediction of intestinal drug absorption. *J. Pharm. Sci.* **2009**, *98*, 2180–2197.

Experimental Section

Chemicals. Quinidine was obtained from Sigma (St. Louis, MO) and the ^{3}H-quinidine was from American Radiolabeled Chemicals (St. Louis, MO). Bafilomycin A1 was from LC Laboratories (Woburn, MA). The P-gp inhibitor GF120918[33] was a kind gift from GlaxoSmithKline (Research Triangle Park, NC). Fetal bovine serum was obtained from EuroClone (U.K.), and other cell culture reagents were from BioWhittaker (Belgium).

Cell Culture. MDCKII-MDR1 (The Netherlands Cancer Institute, Amsterdam, The Netherlands) and Caco-2 (ATCC HTB-37, Manassas, VA) cells were cultured and prepared for permeation experiments as described earlier.[17,34] For permeability experiments, the cells were seeded onto uncoated polycarbonate filters (pore size 0.4 μm, diameter 12 mm; Corning Life Sciences, Corning, NY). MDCKII-MDR1 (passages 34−43) and Caco-2 (passages 42−45) were used for permeation experiments at 4 and 21−24 days postseeding, respectively.

Permeation Experiments and Sample Analysis. The donor solutions with unlabeled quinidine at the concentrations indicated were prepared in the corresponding transport buffer, HBSS buffered with 25 mM Hepes (pH $\geq$ 7.0) or MES (pH < 7.0) with or without 5 μM GF120918, P-gp inhibitor, and/or 100 nM Bafilomycin A1, a specific inhibitor of vacuolar type H^+ -ATPase,[35] that inhibits the acidification of lysosomes[36] and, thus, reduces the cellular retention of lysosomotrophic compounds.[28] The donor solutions were spiked with ^{3}H-quinidine. The stock solutions were prepared in dimethyl sulfoxide, but the dimethyl sulfoxide concentration did not exceed 1% in final donor solutions.

Before the experiments, the cell monolayers were washed and preincubated for 30 min at 37 °C in a humidified incubator in the appropriate transport buffer. The integrity of the monolayers was checked by a transepithelial electrical resistance measurement, only data from inserts with resistance higher than 150 Ω cm^2 (MDCKII-MDR1) or higher than 300 Ω cm^2 (Caco-2) were included in the analysis.

The experiments were started by replacing the preincubation buffer with fresh transport buffer into the receiver chamber and donor solution into the donor chamber. At each sampling time point (5, 15, 30, 45, 60, 90, and 120 min), 25 μL samples were withdrawn from both chambers simultaneously. Additionally, promptly after the final sampling, the filters were washed with ice cold HBSS-Hepes, pH 7.4, and the cells were lysed with 300 μL of HBSS-Hepes, pH 7.4, supplemented with 1% Triton X 100 at least for 30 min at 37 °C in a humidified incubator. The cell lysates were carefully mixed, and 100 μL samples were withdrawn for liquid scintillation counting.

The permeation experiments were conducted at 37 °C in a humidified incubator on an orbital shaker with an orbit diameter of 3 mm or 1.5 mm (small) as indicated (Titramax 101 or Titramax 1000, respectively; Heidolph, Schwabach, Germany). The shaking rate was 320 rpm in all experiments.

In the sample analysis, the samples were mixed with 500 μL of OptiPhase HiSafe scintillation cocktail (PerkinElmer Wallac) and the radioactivity was quantified using a MicroBeta liquid scintillation counter (PerkinElmer Wallac, Turku, Finland).

Selection of Compounds. Quinidine was chosen as the model compound for these studies because it is a well-known P-gp substrate that is stable in the cell monolayer permeation setting and it can readily be used in such experiments in the concentration range where a full saturation curve of the apparent P-gp mediated transport is observed. Furthermore, quinidine has been used as a model compound also in the earlier P-gp studies in our laboratory.[17,37] GF120918 is an effective inhibitor of both P-gp and breast cancer resistance protein (BCRP/ABCG2). In the presence of GF120918 the polarization of quinidine disposition through the cell monolayer is abolished in both cell lines used.[17] Moreover, the evidence available in the literature suggests that quinidine does not interact with BCRP or multidrug resistance-associated protein 2 (MRP2/ABCC2),[38] the other major ABC transporters expressed in the Caco-2 cells as well as in the intestinal epithelia. Thus, although several other transporters are expressed in the cell lines used,[39,40] the data is not expected to be significantly confounded by the involvement of other transporters than P-gp. However, a minor contribution of additional transporters cannot be ruled out totally.

(33) Hyafil, F.; Vergely, C.; Du Vignaud, P.; Grand-Perret, T. In vitro and in vivo reversal of multidrug resistance by GF120918, an acridonecarboxamide derivative. *Cancer Res.* **1993**, *53*, 4595–4602.

(34) Korjamo, T.; Honkakoski, P.; Toppinen, M. R.; Niva, S.; Reinisalo, M.; Palmgren, J. J.; Mönkkönen, J. Absorption properties and P-glycoprotein activity of modified Caco-2 cell lines. *Eur. J. Pharm. Sci.* **2005**, *26*, 266–279.

(35) Bowman, E. J.; Siebers, A.; Altendorf, K. Bafilomycins: a class of inhibitors of membrane ATPases from microorganisms, animal cells, and plant cells. *Proc. Natl. Acad. Sci. U.S.A.* **1988**, *85*, 7972–7976.

(36) Yoshimori, T.; Yamamoto, A.; Moriyama, Y.; Futai, M.; Tashiro, Y. Bafilomycin A1, a specific inhibitor of vacuolar-type H(+)-ATPase, inhibits acidification and protein degradation in lysosomes of cultured cells. *J. Biol. Chem.* **1991**, *266*, 17707–17712.

(37) Heikkinen, A. T.; Mönkkönen, J. Protein concentration and pH affect the apparent P-glycoprotein-ATPase activation kinetics. *Int. J. Pharm.* **2008**, *346*, 169–172.

(38) Matsson, P.; Pedersen, J. M.; Norinder, U.; Bergstrom, C. A.; Artursson, P. Identification of novel specific and general inhibitors of the three major human ATP-binding cassette transporters P-gp, BCRP and MRP2 among registered drugs. *Pharm. Res.* **2009**, *26*, 1816–1831.

(39) Goh, L. B.; Spears, K. J.; Yao, D.; Ayrton, A.; Morgan, P.; Roland Wolf, C.; Friedberg, T. Endogenous drug transporters in in vitro and in vivo models for the prediction of drug disposition in man. *Biochem. Pharmacol.* **2002**, *64*, 1569–1578.

(40) Ahlin, G.; Hilgendorf, C.; Al-Khalili Szigyarto, C.; Uhlen, M.; Karlsson, J. E.; Artursson, P. Endogenous gene and protein expression of drug transporting proteins in cell lines routinely used in drug discovery programs. *Drug Metab. Dispos.* **2009**, *37*, 2275–2283.

Table 1. Summary of Permeation Experiments Conducted To Experimentally Dissect the Roles of Different Factors Affecting the Apparent P-gp Mediated Transport of Quinidine, for the Cell Lines MDCKII-MDR1 and Caco-2[a]

factor probed	exptl approach used	extracellular pH[b]	orbit diam[c] (mm)	treatment
	MDCKII-MDR1			
none		7.4	3	none
aqueous boundary layer	change of agitation scheme	7.4	1.5	none
cell membrane permeability	change of extracellular pH	6.4	3	none
		6.4	1.5	none
cellular retention	inhibn of lysosomal sequestration of quinidine	7.4	3	BAF[d]
		6.4	3	BAF[d]
	Caco-2[e]			
expression level of P-gp	use of cell lines with different P-gp expression levels	7.4	3	none
		6.4	3	none

[a] The experiments were conducted only in the absorptive direction (apical to basal). [b] The same pH was used in both apical and basal compartments. [c] Orbital shaking rate in all experiments was 320 rpm. [d] Lysosomal acidification and consequent lysosomal sequestration of quinidine were inhibited by treating the cells with 100 nM bafilomycin A1. [e] The P-gp expression level in Caco-2 cells is significantly lower than in MDCKII-MDR1 cells (Korjamo et al.[17]).

Determination of the Apparent Permeability and Apparent P-gp Function. To study the effects of different factors on the apparent P-gp mediated transport as well as on the apparent passive permeability of quinidine, the permeation experiments were conducted with six different donor concentrations ranging from 1 to 300 μM in MDCKII-MDR1 or from 0.3 to 100 μM in Caco-2 in the absorptive direction (apical to basal) with and without the P-gp inhibitor, GF120918 (5 μM), at eight different experimental conditions. The experimental approaches to probe the effects of aqueous boundary layer, cell membrane permeability and cellular retention are summarized in Table 1.

The concentration dependency of the effective P-gp mediated transport in permeation setting (absorptive direction) has often been described with eq 1.

$$\frac{dQ}{dt} = P_{app}AC_{d0} = P_{pass}AC_{d0} - V_{max,app}A\frac{C_{d0}}{K_{m,app} + C_{d0}} \quad (1)$$

dQ/dt is the (linear phase) appearance rate of the compound into the receiver compartment under "sink conditions", P_{app} is the apparent permeability, A is the nominal area of the support filter (113.1 mm^2) and C_{d0} is the initial donor concentration. P_{pass} is the apparent passive diffusion based permeability through the whole barrier, and the P-gp mediated transport is described as Michaelis−Menten type kinetics, i.e. $V_{max,app}$ and $K_{m,app}$ parameters, referring to maximum effective P-gp mediated transport rate (per unit area) and the initial donor concentration needed to reach 50% of $V_{max,app}$, respectively. Equation 1 can be modified to solve the concentration dependency of P_{app}.

$$P_{app} = P_{pass} - \frac{V_{max,app}}{K_{m,app} + C_{d0}} \quad (2)$$

Equation 1 was applied to determine P_{app}. Subsequently, eq 2 was fitted to the P_{app} at six quinidine concentrations without P-gp inhibitor to estimate P_{pass}, $V_{max,app}$ and $K_{m,app}$ parameters under different experimental conditions using GraphPad Prism software, version 4.03 (GraphPad Software Inc., San Diego, CA). In order to avoid unreasonably high P_{pass} estimates, P_{pass} was constrained not to be higher than the highest apparent permeability observed at the corresponding experimental conditions (with or without P-gp inhibitor GF120918). Extra sum of squares F test was used for comparison of $V_{max,app}$ and $K_{m,app}$ at different experimental conditions, and P values lower than 0.05 were considered to signify statistically significant difference.

Differential Equations Describing the Three- Compartment Model. Three- compartment model (Figure 1A) adapted from ref 28 was used for estimation of concentration dependency of cellular distribution coefficient K.

$$K = \frac{C_{cell}}{C_{cell,free}} \quad (3)$$

P-gp mediated transport reduces the cellular retention of quinidine and, thus, would confound the estimation of K. Therefore, K was estimated on the basis of experiments conducted in the presence of the P-gp inhibitor, 5 μM GF120918, and a three-compartment model accounting only for passive transfer was applied.

The time profiles of free concentration at apical (C_{api}) and basal (C_{baso}) chambers and in the cell monolayer ($C_{cell,free}$) are defined as

$$\frac{dC_{api}}{dt} = \frac{A}{V_{api}}[-P_{api}(C_{api} - C_{cell,free})] \quad (4)$$

$$\frac{dC_{cell,free}}{dt} = \frac{A}{V_{cell}K}[P_{api}(C_{api} - C_{cell,free}) - P_{baso}(C_{cell,free} - C_{baso})] \quad (5)$$

$$\frac{dC_{baso}}{dt} = \frac{A}{V_{baso}}[P_{baso}(C_{cell,free} - C_{baso})] \quad (6)$$

P_{api} and P_{baso} are the composite permeability coefficients across the ABL and cell membrane at the apical and basal sides, respectively. V_{api} and V_{baso} refer to volumes of apical

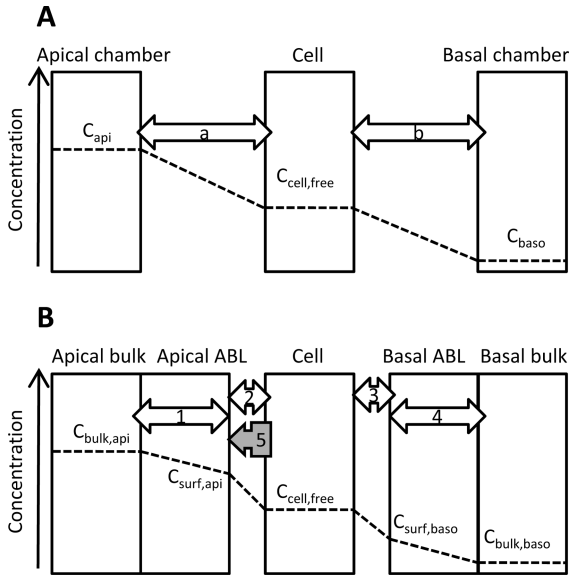

Figure 1. Box model presentation of three-compartment (A) and five-compartment (B) models. The dashed line shows schematically the approximation of the concentration gradient across the donor to receiver compartment in apical to basal direction experiments at pH 7.4. In the three-compartment model the aqueous boundary layer (ABL) and cell membrane at both sides of the cell monolayer are described as single barriers (a, b). The five-compartment model accounts for the ABLs and cell membranes individually (1–4) and allows the inclusion of P-gp mediated efflux through the apical cell membrane (5) into a mechanistically feasible location.

and basal chambers, respectively. The chamber volumes decline stepwise 25 μL at each sampling time. The cellular volume (V_{cell}) for modeling was calculated from the nominal filter area and the height of the cell monolayer estimated from cross sectional microscopy (10 μm for MDCKII-MDR1 and 20 μm for Caco-2). The concentration dependence of the cellular distribution coefficient K[28] is defined as

$$K = K_{max} - (K_{max} - K_{min})\frac{C_{cell,free}}{EC_{50} + C_{cell,free}} \quad (7)$$

EC_{50} refers to the intracellular free concentration resulting in the K of average of upper (K_{max}) and lower (K_{min}) limits.

Differential Equations Describing the Five-Compartment Model. A five-compartment model accounting separately for ABLs, cell membranes and the concentration dependent P-gp mediated transport was constructed. The time profile of average free concentration at apical ($C_{bulk,api}$, $C_{ABL,api}$) and basal ($C_{bulk,baso}$, $C_{ABL,baso}$) bulk and ABL compartments, respectively, and in the cell monolayer ($C_{cell,free}$) are defined as

$$\frac{dC_{bulk,api}}{dt} = \frac{A}{V_{bulk,api}}[-P_{ABL,api}(C_{bulk,api} - C_{surf,api})] \quad (8)$$

$$\frac{dC_{ABL,api}}{dt} = \frac{A}{V_{ABL,api}}[P_{ABL,api}(C_{bulk,api} - C_{surf,api}) - (f_uP_u + f_iP_i)C_{surf,api} + (f_{u,cell}P_u + f_{i,cell}P_i)C_{cell,free} + J_{P\text{-}gp}] \quad (9)$$

$$\frac{dC_{cell,free}}{dt} = \frac{A}{V_{cell}K}[(f_uP_u + f_iP_i)(C_{surf,api} + C_{surf,baso}) - 2(f_{u,cell}P_u + f_{i,cell}P_i)C_{cell,free} - J_{P\text{-}gp}] \quad (10)$$

$$\frac{dC_{ABL,baso}}{dt} = \frac{A}{V_{ABL,baso}}[(f_{u,cell}P_u + f_{i,cell}P_i)C_{cell,free} - (f_uP_u + f_iP_i)C_{surf,baso} - P_{ABL,baso}(C_{surf,baso} - C_{bulk,baso})] \quad (11)$$

$$\frac{dC_{bulk,baso}}{dt} = \frac{A}{V_{bulk,baso}}[P_{ABL,baso}(C_{surf,baso} - C_{bulk,baso})] \quad (12)$$

P-gp mediated transport rate *in situ* is defined as

$$J_{P\text{-}gp} = V_{max}\frac{C_{cell,free}}{K_m + C_{cell,free}} \quad (13)$$

or in the presence of the P-gp inhibitor GF120918

$$J_{P\text{-}gp} = 0 \quad (14)$$

$P_{ABL,api}$ and $P_{ABL,baso}$ are the permeabilities across the apical and basal ABLs, respectively. Current data did not allow for the determination of the permeabilities of un-ionized (P_u) and ionized (P_i) species separately in the apical and basal cell membranes. Thus, equal values were used for both cell membranes. The problematics of distinguishing the permeabilities across the apical and basal cell membranes are further discussed elsewhere (Heikkinen, A.T., Mönkkönen, J., Korjamo, T. Determination of permeation resistance distribution in in vitro cell monolayer permeation experiments. *Eur J Pharm Sci*, in press).

Quinidine is a diprotic base with pK_a values of 4.32 and 8.51,[41] i.e. there are two ionized species of quinidine present at the pH conditions applied. However, current data does not allow determination of permeation characteristics of these two ionized species separately (not shown). Thus, the membrane permeability of both ionized species were approximated to be equal and only the pK_a value of 8.51 was used to calculate the un-ionized and ionized fractions (f_u, f_i and $f_{u,cell}$, $f_{i,cell}$ in extra- and intracellular spaces, respectively).

The operational ABL volumes separately at each side are

$$V_{ABL} = \frac{D_{aq}}{P_{ABL}}A \quad (15)$$

(41) Avdeef, A. Box, K. J. *Sirius Technical Application Notes (STAN)*. Sirius Analytical Instruments Ltd.: Forest Row, U.K., 1995; Vol. 2.

The aqueous diffusion coefficient (D_{aq}) of quinidine at 37 °C (7.16 cm/s × 10^{-6}) was calculated with equations presented in ref 22.

Consequently bulk phase volumes are

$$V_{bulk} = V_{tot} - V_{ABL} \quad (16)$$

V_{tot} refers to the total volume of the corresponding chamber (V_{api} or V_{baso}). The stepwise decline in the volumes due to sampling was taken into account.

The concentrations at the cell surfaces ($C_{surf,api}$ and $C_{surf,baso}$) were estimated from the bulk concentration (C_{bulk}) and the average ABL concentration (C_{ABL}) at the respective side of the cell monolayer assuming a linear concentration gradient within the ABLs.

$$C_{surf} = 2C_{ABL} - C_{bulk} \quad (17)$$

Parameter Estimation. The estimation of parameters describing the quinidine disposition in cell permeation experiments was done by sequential fitting the compartmental models to apical and basal chamber concentration data of several permeation experiments using WinNonlin software, version 5.2.1 (Pharsight, Mountain View, CA). A weighting scheme 1/predicted^2 was chosen based on residual plots and SE of the parameter estimates. Otherwise, the default WinNonlin settings for minimization of error were applied.

In the first fitting step, the parameters describing the concentration dependency of cellular binding of quinidine (K_{max}, K_{min} and EC_{50}) to MDCKII-MDR1 and Caco-2, and to MDCKII-MDR1 in the presence of 100 nM bafilomycin A1 were estimated by fitting the three-compartment model (Figure 1A) to the data from corresponding experiments with six different quinidine concentrations in the presence of 5 μM GF120918 at pH 7.4. When the disposition through individual permeation barriers is symmetric (i.e., when pH gradient across membranes or active transporters are not involved), the apical and basal permeation barriers (including ABL and cell membrane each) can be described as single barriers.[28] Furthermore, at this step there were no separate estimates of ABL and cell membrane permeabilities available. Therefore, the three-compartment model was exploited in this parameter estimation step.

In the second fitting step, the cellular binding parameters were fixed to the best fit values of the first fitting step. Subsequently, the parameters describing the passive permeation through the cell membranes (P_u and P_i) and ABLs ($P_{ABL,api}$ and $P_{ABL,baso}$) were estimated by fitting the five-compartment model (Figure 1B) into the concentration data from permeation experiments through MDCKII-MDR1 into both directions at five different pH values (5.6, 6.0. 6.4, 7.0 and 7.4). The initial donor quinidine concentration was 30 μM, and 5 μM GF120918 was present in both donor and receiver compartments. P_u and P_i were constrained to be independent of agitation, whereas separate values for $P_{ABL,api}$ and $P_{ABL,baso}$ were estimated for experiments conducted under different agitation conditions.

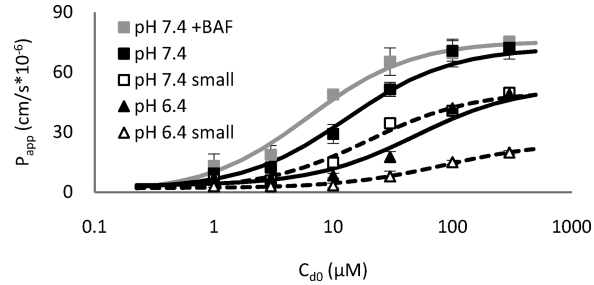

Figure 2. Effect of extracellular pH, aqueous boundary layer and cellular retention on the apparent P-gp mediated transport of quinidine through MDCKII-MDR1 cell monolayers. The symbols refer to the average of three to six measurements (± standard deviation), and the predicted curves are simulated with the best fit values of eq 2. Squares are for pH 7.4 and triangles for pH 6.4. Solid and open symbols represent the experiments on the shakers with 3 mm and 1.5 mm (small) orbit diameter, respectively. Gray color refers to experiments with inhibition of lysosomal sequestration (100 nM bafilomycin A). The results of the experiments in the presence of bafilomycin A at pH 6.4 are not presented for clarity.

In the final, third, fitting step, the passive permeability parameters were fixed to the best fit values of the second fitting step and the cellular binding parameters remained fixed to the corresponding best fit values of the first fitting step. Subsequently, the parameters describing the concentration dependent P-gp mediated transport *in situ* (V_{max} and K_m) were estimated by fitting the five-compartment model to data from experiments with six different quinidine concentrations in the absence of GF120918 at each experimental condition (Table 1).

Results

Effects of Passive Permeability on the Apparent P-gp Mediated Transport. Figure 2 illustrates the effects of extracellular pH and ABL on the concentration dependence of the apparent permeability of quinidine. Quinidine is more ionized at pH 6.4 than at pH 7.4 and, consequently, the permeability through the cell monolayer was lower at pH 6.4 than at pH 7.4, whereas the permeability through ABLs is assumed to be unaffected. Additionally, the change of pH from 7.4 to 6.4 also shifted the P-gp saturation curve to the right (i.e., to higher concentrations). This shift was manifested as the higher apparent $K_{m,app}$. In addition, the apparent $V_{max,app}$ was higher at pH 6.4 than in pH 7.4 (Table 2). Similar pH effects in $K_{m,app}$ and $V_{max,app}$ were observed at both shaking orbits (3 mm and 1.5 mm) and with both cell lines.

Reduced agitation (change of shaking orbit diameter from 3 mm to 1.5 mm) reduced the permeability through ABLs, whereas the permeability through the cell monolayer was assumed to be unaffected. Additionally, the P-gp saturation curve shifted slightly to the right. Although the apparent passive permeability through the whole system was reduced

Table 2. Summary of Fitted Parameters (±SE) from Fitting of Eq 2 to Apparent Permeability Data and from the Compartmental Modeling, for Cell Lines MDCKII-MDR1 and Caco-2

exptl condtns	P_{pass}[c] (cm/s × 10^{-6})	$V_{max,app}$[c] (fmol/s/cm^2)	$K_{m,app}$[c] (μM)	$P_{ABL,api}$[d] (cm/s × 10^{-6})	$P_{ABL,baso}$[d] (cm/s × 10^{-6})	P_u[d] (cm/s × 10^{-6})	P_i[d] (cm/s × 10^{-6})	K_{max}[e]	K_{min}[e]	EC_{50}[e] (μM)	V_{max}[f] (fmol/s/cm^2)	K_m[f] (μM)
					MDCKII-MDR1							
pH 7.4	72 ± 2	920 ± 90[g]	13 ± 2[g]	440 ± 40	170 ± 8	26700 ± 1300	21 ± 3	538 ± 12	89 ± 5	1.2 ± 0.1	5670 ± 300	0.23 ± 0.02
pH 6.4	53 ± 3	2450 ± 240[g,h]	49 ± 5[g,h]								4910 ± 190	0.28 ± 0.01
pH 7.4 + BAF[a]	76 ± 2	470 ± 60[i]	6 ± 1[i]					53 ± 3	47 ± 6	16 ± 62	4710 ± 220	0.22 ± 0.02
pH 6.4 + BAF[a]	59 ± 3	2080 ± 220[h]	40 ± 5[h]								3930 ± 230	0.36 ± 0.03
pH 7.4 small[b]	50 ± 2	980 ± 110	20 ± 3	200 ± 12	87 ± 2			538 ± 12	89 ± 5	1.2 ± 0.1	7490 ± 550	0.28 ± 0.03
pH 6.4 small[b]	25 ± 1	1960 ± 110[h]	85 ± 6[h,j]								8090 ± 420	0.27 ± 0.03
					Caco-2							
pH 7.4	69 ± 2	470 ± 40	9 ± 1	440 ± 40	170 ± 8			233 ± 6	77 ± 4	0.6 ± 0.1	1970 ± 120	0.28 ± 0.02
pH 6.4	56 ± 5	1340 ± 160[h]	31 ± 4[h]								3210 ± 140	0.30 ± 0.03

[a] Lysosomal sequestration was inhibited by neutralizing the lysosomes with 100 nM bafilomycin A1. [b] "Small" refers to the experiments conducted on the orbital shaker with 1.5 mm orbit diameter. All the other experiments were on the orbital shaker with 3 mm orbit diameter. [c] Parameters describing the apparent passive permeability through the cell membrane and concentration dependence of apparent effective P-gp mediated transport were estimated by fitting the apparent permeability data into eq 2. [d] Parameters describing the passive permeation of ionized and un-ionized quinidine through ABLs and cell membranes were estimated on the second step of sequential compartmental model fitting. [e] Parameters describing the concentration dependence of cellular binding were estimated on the first step of sequential compartmental model fitting. [f] Parameters describing the concentration dependence of P-gp mediated transport *in situ* were estimated on the third step of sequential compartmental model fitting. [g] Significantly higher for MDCKII-MDR1 than for Caco-2 at similar experimental conditions. [h] Significantly higher values at pH 6.4 than at pH 7.4 at otherwise similar experimental conditions. [i] Significantly lower than the corresponding value without bafilomycin A. [j] Significantly higher at small shaker.

Figure 3. The effects of P-gp mediated efflux, lysosomal sequestration and extracellular pH on the extent of cellular retention of quinidine in permeation experiments. The symbols refer to the amount of quinidine recovered from the MDCKII-MDR1 cell monolayer at the end of the permeation experiments (at 120 min) at pH 7.4 (A) and at pH 6.4 (B) (average of three to six measurements ± standard deviation). Solid symbols/thick lines refer to experiments with 5 μM GF120918 (P-gp inhibitor), and open symbols/thin lines refer to experiments without GF120918. Triangles/dashed lines refer to experiments with 100 nM bafilomycin A (inhibition of lysosomal sequestration) and squares/solid lines refer to experiments without bafilomycin A.

virtually to the same extent by the change in the cell monolayer permeability (the pH effect at 3 mm shaker) and by the change in ABL permeability (the agitation effect at pH 7.4), the shift in the P-gp saturation curve was less pronounced in the latter case (Figure 2). Consequently, $V_{max,app}$ remained virtually unaffected by the agitation and there was a tendency toward the higher $K_{m,app}$ values at reduced agitation. Similar effects in $K_{m,app}$ and $V_{max,app}$ due to agitation applied were observed at both pH conditions (6.4 and 7.4). However, the effect on $K_{m,app}$ reached statistical significance only at pH 6.4 (Table 2).

Effects of Lysosomal Sequestration on the Apparent P-gp Mediated Transport. Weak bases, such as quinidine, are susceptible to lysosomal sequestration during permeation experiments.[28] Consequently, the inhibition of the acidification of lysosomes by bafilomycin A1 reduced the extent of cellular retention of quinidine at pH 7.4 (Figure 3).

At low quinidine concentrations P-gp efficiently reduced the cellular retention of quinidine. At intermediate quinidine concentrations, the P-gp started to saturate and the cellular retention increased, whereas at high quinidine concentrations, the cellular retention again decreased probably because of the saturation of cellular binding and lysosomal sequestration of quinidine (Figure 3). A similar bell shape trend in cellular retention as a function of quinidine concentrations was observed with each experimental setup. However, this trend was less pronounced in the presence of bafilomycin A and in the pH 6.4 experiments because of the lower cellular retention (Figure 3B). Consequently, quinidine was retained in the cells to a greater extent at intermediate concentrations than at low or high concentrations and the effect of bafilomycin A on cellular retention was most pronounced at intermediate concentrations. Cellular retention decreases the appearance rate into the receiver compartment and, thus, decreases the apparent permeability.[28] Consequently, the inhibition of lysosomal sequestration caused an increase in P_{app} at the intermediate quinidine concentrations whereas the P_{app} at high and low quinidine concentrations was affected to a markedly lesser extent. Consequently, at pH 7.4 the apparent P-gp saturation curve shifted to the left in the presence of bafilomycin A1 (Figure 2). This was reflected as significantly lower apparent $K_{m,app}$ and $V_{max,app}$ values (Table 2).

At pH 6.4, the extent of cellular retention was significantly lower than at pH 7.4 (Figure 3). Therefore, the cellular retention and the effect on the cellular retention by bafilomycin A1 did not significantly affect the apparent permeability of quinidine. Consequently, the $K_{m,app}$ and $V_{max,app}$ values were not significantly affected by bafilomycin A1 at pH 6.4 (Table 2). This suggests that bafilomycin A1 did not have any direct effect on P-gp function but, rather, the effect seen at pH 7.4 was caused by the changes in the cellular retention.

Effects of P-gp Expression Level on the Apparent P-gp Mediated Transport. Comparison of the concentration dependent apparent permeability through MDCKII-MDR1 and Caco-2 monolayers is shown in Figure 4. Caco-2 cells have a lower P-gp expression level than MDCKII-MDR1 cells, whereas the passive permeability of quinidine is apparently rather similar in both of these cell lines[17] (Figure 4, Table 2). The effect of P-gp mediated transport on the apparent permeability of quinidine was more pronounced in MDCKII-MDR1 cells than in Caco-2 cells as expected based on P-gp expression levels. This was reflected as higher $V_{max,app}$ and $K_{m,app}$ values in MDCKII-MDR1 cells compared to Caco-2 cells (Table 2).

Compartmental Modeling and Determination of K_m and V_{max} of P-gp Mediated Transport *in Situ*. The estimated parameters from sequential compartmental model fitting are summarized in Table 2. Additionally, comparisons of $K_{m,app}$ and $V_{max,app}$ and *in situ* K_m and V_{max} values of P-gp mediated transport of quinidine at different experimental setups are visualized in Figure 5. The K_m values at different setups were all at a similar level, the average being 0.3 μM

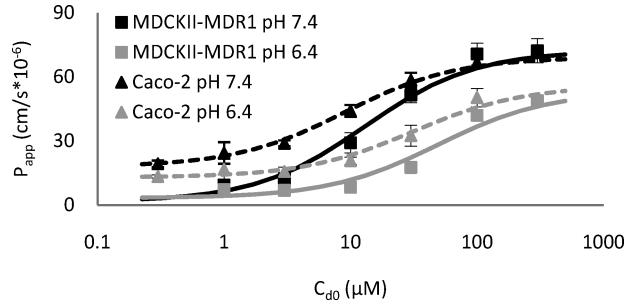

Figure 4. Effect of P-gp expression level on the apparent P-gp mediated transport of quinidine. The symbols refer to average of three to six measurements (± standard deviation), and the predicted curves are simulated with the best fit values of eq 2. Squares/solid lines and triangles/dashed lines refer to MDCKII-MDR1 and Caco-2, respectively. Black and gray color refer to pH 7.4 and 6.4, respectively.

with 1.6-fold difference between the lowest and highest estimates, whereas the $K_{m,app}$ values varied by more than 1 order of magnitude. The relative variation in V_{max} estimates between different experimental settings was larger than in K_m estimates and, thus, partly masking the presumed difference in V_{max} between Caco-2 and MDCKII-MDR1. However, on average, the V_{max} estimates in MDCKII-MDR1 (5800 fmol/s/cm^2) were almost 3-fold higher than those obtained with Caco-2 (2100 fmol/s/cm^2). Furthermore, the $K_{m,app}$ estimates were significantly higher than *in situ* K_m values whereas $V_{max,app}$ values were significantly lower than their *in situ* V_{max} counterparts. The difference between $K_{m,app}$ and K_m values was more pronounced at pH 6.4 than at pH 7.4 and also slightly more pronounced in experiments with the 1.5 mm shaker than in experiments with the 3 mm shaker, whereas the difference between $V_{max,app}$ and V_{max} was more pronounced at pH 7.4 than at pH 6.4 and at a similar level with both agitation conditions.

Discussion

The apparent active transporter kinetics in *in vitro* permeation experiments are usually biased by the experimental setup and the combination of both active and passive permeation. This study examined the effects of the experimental setup on the apparent kinetic parameters of the P-gp mediated transport. The expression level of P-gp and, consequently, the P-gp mediated transport rate have been reported to be higher in MDCKII-MDR1 cells than in Caco-2 cells.[17,18] Furthermore, the P-gp mediated transport decreases the substrate concentration at the intracellular binding site of P-gp, and thus, the higher the level of expression is, the higher an initial donor concentration is needed to saturate the pump, i.e. a higher $K_{m,app}$.[17,20] The values of both $V_{max,app}$ and $K_{m,app}$ observed in this study under similar experimental conditions were higher in MDCKII-MDR1 cells than their counterparts in Caco-2, thus supporting the results reported earlier. Furthermore, both $V_{max,app}$ and $K_{m,app}$ observed in this study were higher at extracellular pH 6.4 than at pH 7.4. Thus, the effects of the extracellular pH on the apparent

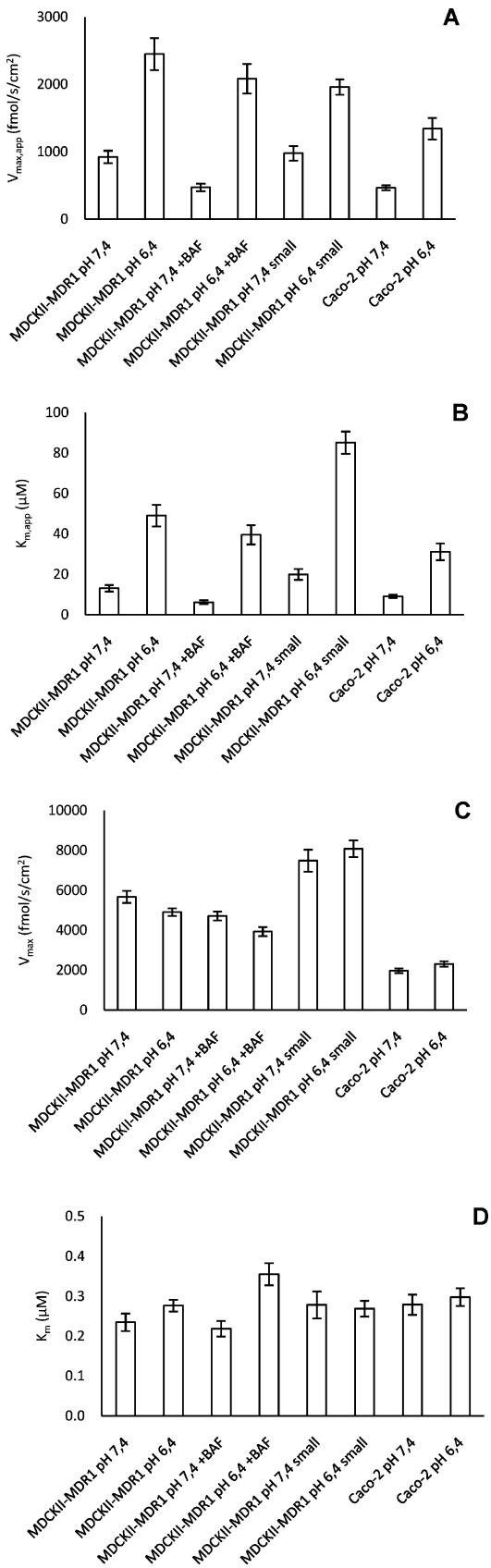

Figure 5. The apparent (A, B) and *in situ* (C, D) parameters describing the concentration dependent P-gp mediated transport of quinidine at different experimental conditions.

concentration dependent P-gp mediated transport of quinidine are also in line with the results reported earlier in the literature.[21] Additionally, the permeation resistance of ABL and the cellular retention were demonstrated to play a role in the apparent concentration dependent P-gp mediated transport of quinidine. However, the compartmental modeling results indicate that the P-gp function *per se* was not affected by the experimental conditions but, rather, the changes seen in the apparent P-gp kinetics were due to the modulation of the access of the substrate to the binding site of the transporter protein.

P-gp transports the substrate molecules out of the cell across the apical cell membrane. Thus, P-gp mediated transport reduces the permeation rate through the cell monolayer in absorptive direction permeation experiments by maintaining the concentration gradient across the apical cell membrane. In contrast, the permeabilities across the other permeation barriers (i.e., ABL at both sides of the cell monolayer and the basal cell membrane) are not affected by P-gp. The magnitude of the concentration gradient across the apical cell membrane maintained by P-gp and, consequently, the effective P-gp mediated transport rate are dictated by the actual P-gp mediated transport rate and the passive permeation rate from the apical cell surface to the intracellular binding site of P-gp. Thus, the maximum effective transport rate ($V_{max,app}$) is increased by the maximum actual transport rate (i.e., V_{max}) and decreased by the passive permeability through the apical cell membrane from the cell surface into the cell (i.e., $f_iP_i + f_uP_u$). Consequently, $V_{max,app}$ is bound to be lower than V_{max}. Lowering the extracellular pH decreases the passive permeability of quinidine from the cell surface into the cell whereas the P-gp function *per se* is believed not to be affected by the pH conditions.[37,42] This is seen as higher $V_{max,app}$ at 6.4 compared to the situation at 7.4 (Table 2, Figure 5). In contrast, decreasing the permeability through the whole cell monolayer by decreasing the agitation (i.e., decreasing the ABL permeability) does not affect the passive permeability from the cell surface into the cell nor the P-gp function. Consequently, the $V_{max,app}$ is not significantly affected by the agitation applied (Table 2, Figure 5).

$K_{m,app}$ represents the initial donor concentration resulting in 50% of $V_{max,app}$. Thus, $K_{m,app}$ is a composite parameter representing the actual K_m as well as the relationship of the initial donor concentration and the concentration at the intracellular binding site of P-gp. $K_{m,app}$ is bound to be higher than K_m because the intracellular binding site of P-gp is downstream from the donor compartment in the concentration gradient. The changes applied in the experimental setup are assumed not to affect the actual K_m. Thus, all the variation in $K_{m,app}$ can be attributed to the changes in the access to the intracellular binding site of P-gp. The decrease in the

(42) Altenberg, G. A.; Young, G.; Horton, J. K.; Glass, D.; Belli, J. A.; Reuss, L. Changes in intra- or extracellular pH do not mediate P-glycoprotein-dependent multidrug resistance. *Proc. Natl. Acad. Sci. U.S.A.* **1993**, *90*, 9735–9738.

permeability from the donor bulk phase into the intracellular binding site of P-gp by either lowering the extracellular pH or decreasing the agitation reduces the access rate of the substrate to the binding site of P-gp. Consequently, the initial donor concentration needed to saturate the pump is increased, i.e. the $K_{m,app}$ is increased. However, the decrease in the extracellular pH also increases the effective P-gp mediated transport rate from the binding site. Thus, the concentration gradient in between the donor bulk phase and the intracellular binding site of P-gp is more increased by the decrease in the extracellular pH than by the decrease in the agitation. Consequently, the effect of extracellular pH on the $K_{m,app}$ value is more pronounced than the effect of agitation.

The estimation of $V_{max,app}$ and $K_{m,app}$ is based on P_{app} determined at several substrate concentrations. Since the determination of P_{app} is based on the assumption of 100% recovery, the P_{app} estimates are affected by the recovery.[28] Low recovery (due to e.g. cellular retention) leads to the underestimation of the actual permeability. Consequently, the changes in the recovery as a function of concentration result in concentration dependency of P_{app}. At pH 7.4, the changes in the cellular retention of quinidine, caused by the saturation of P-gp followed by the saturation of apparent cellular binding, were sufficient to cause a shift in the concentration dependence of quinidine P_{app} (Figures 2 and 3). The inhibition of the lysosomal sequestration decreases significantly the cellular retention of quinidine, thus virtually abolishing the concentration dependence of cellular retention and consequently the bias in the apparent saturation of the effective P-gp mediated transport. Although the effects of poor recovery on the P_{app} estimates are generally acknowledged, there are no universal correction terms available for accounting for poor recovery in the determination of P_{app}.[28,43] If there is no evidence of major recovery problems, the effects of recovery are often neglected in the data analysis. However, the results of this study demonstrate that neglecting the role of recovery may bias the interpretation of the apparent concentration dependent transporter function.

It is evident that the single-barrier view based analysis of the apparent concentration dependency of P-gp mediated transport is biased by the passive disposition of the compound. Therefore, compartmental modeling was applied to account for the passive disposition and to estimate the P-gp kinetics *in situ*. The estimation of the parameter values embedded in the compartmental model was conducted by sequential fitting of the models to the experimental data. One major drawback of this approach is the fact that the possible misspecifications of the model in the early fitting steps may be reflected in the later fitting steps. On the other hand, the possible misspecifications of the model in the late fitting steps will not confound the early fitting steps. More importantly, for the further application of compartmental models to quantify the concentration dependent transporter function, it would not be feasible to perform all the experiments performed in this study. For instance, the estimates of ABL permeabilities can theoretically be derived from the results of calibrator molecule(s)[44] or the parameters describing the distribution/binding into cellular structures could be derived from separate, simpler experiments.[45,46] This kind of approach would be essentially similar to the current sequential fitting approach. However, determining the optimal study design will require further research.

The *in situ* V_{max} and K_m are considered to reflect the actual P-gp mediated transport kinetics through the apical cell membrane from the intracellular aqueous phase to the cell surface. Thus, V_{max} would be expected to correlate with the expression level of functional P-gp in the cell line used, whereas K_m should be independent of the P-gp expression level. Furthermore, it is assumed that the experimental conditions will not affect the P-gp function *per se*, i.e. K_m and V_{max} should be independent of the experimental conditions. However, the determination of *in situ* K_m is based on the estimated intracellular free concentration of the substrate, i.e. unbound concentration in the cellular aqueous phase, whereas the binding site(s) of P-gp are generally considered to lie within the inner leaflet of the cell membrane.[16] Assuming the association and dissociation rates between the lipid and aqueous phases is much faster than the rate of transmembrane transfer,[45] the concentration at the binding site of P-gp is at constant proportion to the unbound aqueous concentration. Consequently, the current model is consistent with the substrate binding from the lipid phase. However, the K_m determined actually represents the product of the cytosol−cell membrane distribution coefficient and the actual "lipid-phase K_m". There are differences in the cell membrane lipid composition between cells from different tissues.[47] Thus, it can be hypothesized that K_m values might be cell type specific if there are significant differences in the cytosol−cell membrane distribution of the P-gp substrate in different cell types. However, there were no signs of this kind of difference between MDCKII-MDR1 and Caco-2 cell lines.

The K_m estimates were at the same level regardless of the experimental conditions or the cell line utilized (Figure 5, Table 2), thus fulfilling the above-mentioned expectations and providing further confidence on the interpretation of this

(43) Hubatsch, I.; Ragnarsson, E. G.; Artursson, P. Determination of drug permeability and prediction of drug absorption in Caco-2 monolayers. *Nat. Protoc.* **2007**, *2*, 2111–2119.

(44) Yu, H.; Sinko, P. J. Influence of the microporous substratum and hydrodynamics on resistances to drug transport in cell culture systems: calculation of intrinsic transport parameters. *J. Pharm. Sci.* **1997**, *86*, 1448–1457.

(45) Tran, T. T.; Mittal, A.; Aldinger, T.; Polli, J. W.; Ayrton, A.; Ellens, H.; Bentz, J. The elementary mass action rate constants of P-gp transport for a confluent monolayer of MDCKII-hMDR1 cells. *Biophys. J.* **2005**, *88*, 715–738.

(46) Sun, H.; Zhang, L.; Chow, E. C.; Lin, G.; Zuo, Z.; Pang, K. S. A catenary model to study transport and conjugation of baicalein, a bioactive flavonoid, in the Caco-2 cell monolayer: demonstration of substrate inhibition. *J. Pharmacol. Exp. Ther.* **2008**, *326*, 117–126.

(47) Avdeef, A. *Absorption and Drug Development: Solubility, Permeability and Charge State*. Wiley-Interscience: Hoboken, NJ, 2003.

parameter. In addition, the V_{max} estimates within both cell lines were approximately at the same level irrespective of the experimental conditions. However, there was a substantial variation in V_{max} estimates probably partly masking the expected difference between V_{max} in MDCKII-MDR1 and Caco-2. Earlier Western blot results in our lab suggest that the P-gp expression level in MDCKII-MDR1 is about 1 order of magnitude higher than in Caco-2[17] whereas the difference was on average only about 3-fold in V_{max} estimated in this study. The reason(s) for this discrepancy are not known, but several possible explanations can be hypothesized. (A) The P-gp expression levels were not quantified from the cell batches used in this study. Furthermore, for practical reasons, the serum batch used in the cell culture during this study was not the same as utilized in our earlier study. Consequently, the P-gp expression levels reported earlier may not exactly reflect the expression levels in the cells used here. The difference in $K_{m,app}$ and $V_{max,app}$ between MDCKII-MDR1 and Caco-2 in this study was not as significant as in our previous study,[17] thus favoring this explanation. (B) The expression levels quantified by Western blot measure the total expression level of P-gp protein whereas some of the P-gp expressed may not be localized on the cell membrane.[48] Thus, the difference in the P-gp expression levels detected by Western blot may not directly reflect the difference in the expression of active P-gp. (C) There are indications that the permeability is lower across the apical than the basal cell membrane.[49,50] However, the passive permeability coefficients through the apical and basal cell membranes were assumed to be equivalent because the experimental data did not allow for fitting of separate permeability coefficients for the apical and basal cell membranes. Thus, the interplay of passive permeation and P-gp mediated transport through the apical cell membrane may be inaccurately described in the current analysis. (D) The analysis in the current compartmental model was based on the assumption that the passive permeability parameters determined using MDCKII-MDR1 data describe the passive permeation also in Caco-2. This is a reasonable approximation because there were no significant differences between these cell lines in the apparent passive permeabilities at different pH conditions (Figure 4, Table 2). However, the composition of cell membranes as well as other cellular structures is different in these cell lines. Consequently, the assumption of exactly the same permeability coefficients may not be totally correct and this inaccuracy may be translated into the estimated parameters describing the P-gp function.

The pharmacokinetics is a result of the interplay of several mechanisms, such as passive permeability, active transport by several transporters and metabolism in the enterocytes in the case of intestinal absorption. Consequently, successful prediction of the *in vivo* pharmacokinetics based on *in vitro* data, i.e. IVIVE, requires inclusion of all the clinically significant mechanisms and their interplay into a single prediction in both a physiological and mechanistically reasonable way. In practice, several studies aiming for physiologically based IVIVE with varying levels of mechanistic detail have been published in the recent literature.[31,32,51,52] Some of these studies have utilized commercial software designed for this purpose, such as GastroPlus (Simulations Plus Inc., Lancaster, CA) and Simcyp Population-based ADME Simulator (Simcyp Ltd., Sheffield, U.K.). Physiologically based IVIVE of hepatic metabolism have resulted in predictions with sufficient reliability to have practical utility in drug development,[53,54] whereas there are still no success stories published of the IVIVE of concentration dependent efflux transporter kinetics.

The virtually linear correlation between P-gp expression level and both $V_{max,app}$ and $K_{m,app}$, in constant experimental conditions, has been reported recently.[17,18] Consequently, it was suggested that the $V_{max,app}$ and $K_{m,app}$ determined using at least three cell lines with different P-gp expression levels in combination with a scaling factor derived from the apparent passive permeabilities *in vitro* and *in vivo* could be exploited for predicting *in vivo* $V_{max,app}$ and $K_{m,app}$. Subsequently, these estimates could be used for prediction of concentration dependent intestinal wall permeability *in vivo*.[55] However, the results shown in the current study suggest that when the data analysis is based on the apparent permeability as a function of the initial donor concentration, the interpretation of the relationship between passive permeation and P-gp mediated transport is not always straightforward, thus making the extrapolation less reliable. Second, and more importantly, there are often multiple saturable processes affecting the overall permeation through the intestinal wall, such as different transporters and metabolic enzymes. The local concentration at the binding site of an individual transporter may be significantly affected by the

(48) Porcelli, L.; Lemos, C.; Peters, G. J.; Paradiso, A.; Azzariti, A. Intracellular trafficking of MDR transporters and relevance of SNPs. *Curr. Top. Med. Chem.* **2009**, *9*, 197–208.

(49) Ito, S.; Woodland, C.; Sarkadi, B.; Hockmann, G.; Walker, S. E.; Koren, G. Modeling of P-glycoprotein-involved epithelial drug transport in MDCK cells. *Am. J. Physiol.* **1999**, *277*, F84–96.

(50) Gonzalez-Alvarez, I.; Fernandez-Teruel, C.; Garrigues, T. M.; Casabo, V. G.; Ruiz-Garcia, A.; Bermejo, M. Kinetic modelling of passive transport and active efflux of a fluoroquinolone across Caco-2 cells using a compartmental approach in NONMEM. *Xenobiotica* **2005**, *35*, 1067–1088.

(51) Yang, J.; Jamei, M.; Yeo, K. R.; Tucker, G. T.; Rostami-Hodjegan, A. Prediction of intestinal first-pass drug metabolism. *Curr. Drug Metab.* **2007**, *8*, 676–684.

(52) De Buck, S. S.; Mackie, C. E. Physiologically based approaches towards the prediction of pharmacokinetics: in vitro-in vivo extrapolation. *Expert Opin. Drug Metab. Toxicol.* **2007**, *3*, 865–878.

(53) Fagerholm, U. Prediction of human pharmacokinetics--evaluation of methods for prediction of hepatic metabolic clearance. *J. Pharm. Pharmacol.* **2007**, *59*, 803–828.

(54) Rostami-Hodjegan, A.; Tucker, G. T. Simulation and prediction of in vivo drug metabolism in human populations from in vitro data. *Nat. Rev. Drug Discovery* **2007**, *6*, 140–148.

(55) Shirasaka, Y.; Masaoka, Y.; Kataoka, M.; Sakuma, S.; Yamashita, S. Scaling of in vitro membrane permeability to predict P-glycoprotein-mediated drug absorption in vivo. *Drug Metab. Dispos.* **2008**, *36*, 916–922.

interplay with the other transporters and metabolic enzymes. Thus, the applicability of this single-barrier view based scaling of $V_{max,app}$ and $K_{m,app}$ values is limited. For more general applicability of IVIVE, the models used for simulation of *in vivo* kinetics should enable prediction of the interplay of passive diffusion, transporters, metabolic enzymes etc. in the intestinal absorption. Consequently, many recent physiologically based intestinal absorption models have included enterocytes as a distinct kinetic compartment in between the intestinal lumen and the mesenteric circulation.[32,56,57] However, one of the major challenges of using these models for IVIVE is obtaining suitable input parameters which accurately describe the active transporter kinetics.[14,31,32] It is clear that the *in situ* K_m and V_{max} values obtained in this study are to some extent composite parameters that may partly reflect the passive disposition kinetics of the substrate rather than exclusively P-gp mediated transport. However, the robustness against the changes in the experimental conditions suggests that the *in situ* K_m and V_{max} values are not significantly biased by the passive disposition of the substrate. Therefore, compartmental model based quantification of active transporter kinetics seems a promising approach for handling the *in vitro* component of physiologically based IVIVE. However, further research will be needed to confirm this hypothesis.

(56) Huang, W.; Lee, S. L.; Yu, L. X. Mechanistic Approaches to Predicting Oral Drug Absorption. *AAPS J.* **2009**, *11*, 217–224.
(57) Agoram, B.; Woltosz, W. S.; Bolger, M. B. Predicting the impact of physiological and biochemical processes on oral drug bioavailability. *Adv. Drug Delivery Rev.* **2001**, *50* (1), S41–67.

Acknowledgment. The authors thank Dr. Sanna Pasonen-Seppänen for her help with the cross sectional microscopy to estimate the height of the cell monolayers and Markku Taskinen for excellent technical assistance. The authors thank Dr. Ewen MacDonald for his comments on English language in the manuscript. This study was funded by the Finnish Funding Agency for Technology and Innovation (TEKES) and the Graduate School in Pharmaceutical Research.

MP9003089